Article

Abnormal development and dysconnectivity of distinct thalamic nuclei in patients with 22q11.2 deletion syndrome experiencing auditory hallucinations

MANCINI, Valentina, *et al*.

Abstract

Several studies in patients with schizophrenia have demonstrated an abnormal thalamic volume and thalamocortical connectivity. Specifically, hyperconnectivity with somatosensory areas has been related to the presence of auditory hallucinations (AHs). The 22q11.2 deletion syndrome is a neurogenetic disorder conferring proneness to develop schizophrenia, and deletion carriers (22qdel carriers) experience hallucinations to a greater extent than the general population.

Reference

MANCINI, Valentina, *et al*. Abnormal development and dysconnectivity of distinct thalamic nuclei in patients with 22q11.2 deletion syndrome experiencing auditory hallucinations. *Biological Psychiatry*, 2020

DOI : 10.1016/j.bpsc.2020.04.015
PMID : 32620531

Biological Psychiatry: CNNI

Archival Report

Abnormal Development and Dysconnectivity of Distinct Thalamic Nuclei in Patients With 22q11.2 Deletion Syndrome Experiencing Auditory Hallucinations

Valentina Mancini, Daniela Zöller, Maude Schneider, Marie Schaer, and Stephan Eliez

ABSTRACT

BACKGROUND: Several studies in patients with schizophrenia have demonstrated an abnormal thalamic volume and thalamocortical connectivity. Specifically, hyperconnectivity with somatosensory areas has been related to the presence of auditory hallucinations (AHs). The 22q11.2 deletion syndrome is a neurogenetic disorder conferring proneness to develop schizophrenia, and deletion carriers (22qdel carriers) experience hallucinations to a greater extent than the general population.

METHODS: We acquired 442 consecutive magnetic resonance imaging scans from 120 22qdel carriers and 110 control subjects every 3 years (age range: 8–35 years). The volume of thalamic nuclei was obtained with FreeSurfer and was compared between 22qdel carriers and control subjects and between 22qdel carriers with and without AHs. In a subgroup of 76 22qdel carriers, we evaluated the functional connectivity between thalamic nuclei affected in patients experiencing AHs and cortical regions.

RESULTS: As compared with control subjects, 22qdel carriers had lower and higher volumes of nuclei involved in sensory processing and cognitive functions, respectively. 22qdel carriers with AHs had a smaller volume of the medial geniculate nucleus, with deviant trajectories showing a steeper volume decrease from childhood with respect to those without AHs. Moreover, we showed an aberrant development of nuclei intercalated between the prefrontal cortex and hippocampus (the anteroventral and medioventral reuniens nuclei) and hyperconnectivity of the medial geniculate nucleus and anteroventral nucleus with the auditory cortex and Wernicke's area.

CONCLUSIONS: The increased connectivity of the medial geniculate nucleus and anteroventral nucleus to the auditory cortex might be interpreted as a lack of maturation of thalamocortical connectivity. Overall, our findings point toward an aberrant development of thalamic nuclei and an immature pattern of connectivity with temporal regions in relation to AHs.

Keywords: Auditory cortex, Medial geniculate nucleus, Nucleus reuniens, Psychosis, Thalamocortical comaturation, Wernicke's area

https://doi.org/10.1016/j.bpsc.2020.04.015

Of the many structures of the brain potentially involved in the pathophysiology of schizophrenia, the thalamus is uniquely poised to explain the coexistence of higher-order cognitive dysfunctions and sensory processing abnormalities (1–3). Indeed, the thalamus is the principal relay for sensory inputs, and there is also increasing evidence for a role of the anterior thalamic nuclei in cognitive functions such as working memory (4,5). Moreover, the thalamus is thought to have a regulatory role in maintaining the connectivity within and across cortical regions (4) and might mediate the relationship between sensory and cognitive abnormalities (1). Auditory hallucinations (AHs) are defined as the perception of sounds without any external sensory input and are among the most prominent symptoms in schizophrenia (6). A lack of synchronization between networks involved in sensory processing and top-down control may have a key role in the phenomenology of AHs (1).

Although extremely typical of schizophrenia and psychosis, AHs can happen in the context of other psychiatric or neurological diseases comprising focal brain lesions located in the temporal cortices or thalamus (7–10). Consequently, the underlying neurobiology of AHs might be at the crossroads between pathways of structural and dynamic brain alterations leading to different pathologies (9). In this sense, a better understanding of the abnormalities characterizing patients having AHs might help to identify the point of convergence of these pathways leading to a brain state that is necessary, but not sufficient, to experience the symptoms.

ISSN: 2451-9022

It has been hypothesized that AHs might take place in the context of a generalized failure of the brain to attenuate sensory input processing (6). Such impairment in filtering and attributing the right salience to environmental information has been elucidated with electroencephalography paradigms aimed at assessing sensory gating. Indeed, many studies showed a correlation between the extent of sensory gating impairment and the frequency and severity of AHs (11,12). Strikingly, sensory gating was further decreased in a group of patients with schizophrenia during active AHs with respect to the condition without symptoms (13), suggesting that impaired auditory filtering at the thalamic level has a pivotal role in the generation of AHs. Previous literature investigating the neural underpinnings of AHs in schizophrenia has moreover shown an increased sensitivity of the auditory cortex (AC) to its thalamic afferents (14) and functional hyperactivity of the AC during rest measured with different neuroimaging techniques (9,15–22). Likewise, an increased thalamocortical connectivity with the AC has been highlighted in patients with schizophrenia experiencing AHs (14,23). Furthermore, a large study using different functional magnetic resonance imaging (fMRI) paradigms proved that thalamocortical hyperconnectivity is a neural signature of high vulnerability to psychosis (24). Interestingly, translational studies on animal models of schizophrenia confirmed this pattern, demonstrating abnormal thalamocortical projections from the medial geniculate nucleus (MGN) to the AC (25). Overall, a hyperactivity throughout the auditory pathway seems to underlie AHs.

Besides increased thalamocortical connectivity to the AC, anomalies in the structure of the thalamus have been reported, with patients with schizophrenia having remarkably lower volumes of subcortical structures, including the thalamus (26). The atrophy of the thalamus is supposed to happen early in the disease, with patients at the first episode of schizophrenia already showing either a selective impairment of distinct thalamic regions or an overall smaller thalamic volume with respect to the general population (27–30), which further worsens over time (31). Moreover, the rate and frequency of hallucinations have been correlated with the volume reduction of the thalamus (30,32). Such lower thalamic volume has been further causally linked to the hyperconnectivity with the AC under the hypothesis that the latter might happen as a compensatory response to the gray matter impairment (14). However, so far these findings have not been consistently replicated in the same cohort of patients, and there is a relative scarceness of studies investigating the different nuclei of the thalamus, especially from a functional perspective (33). Structural imaging and postmortem studies exploring thalamic nuclei abnormalities pointed to a decreased volume of the anterior thalamic nuclei, the mediodorsal group, and the pulvinar in patients with schizophrenia (1–3).

The extant evidence from these studies, together with the anatomical heterogeneity of thalamic nuclei, strongly suggests the need to explore the structure and function of single thalamic nuclei (2,34) in order to disentangle the contribution of different groups of nuclei to the pathophysiology of hallucinations. To this aim, a new segmentation technique allows the delineation of single thalamic nuclei (35), comprising subregions that were incorporated into broader ensembles of nuclei in previous procedures for topographic localization.

Patients with a full-blown psychotic disorder have symptoms and brain-related anomalies due to the chronicity of the disease that might interfere with the neuroimaging findings. Hence, studies on individuals at clinical or genetic risk for schizophrenia are aimed at capturing the earliest brain abnormalities without confounding factors related to the progression of the disease (36,37). A population especially suited to be a model to investigate AHs is that of individuals with 22q11.2 deletion syndrome (22q11DS). 22q11DS confers a 25-fold heightened risk of developing schizophrenia with respect to the general population, together with other somatic, cognitive, and psychiatric comorbidities (38–40). More than 30% of deletion carriers (22qdel carriers) meet the criteria for positive subthreshold psychotic symptoms, and notably there is a high prevalence of hallucinations that tend to emerge at an early age (41–44). Therefore, exploring brain structure and function in 22qdel carriers could help to increase our mechanistic understanding of AHs.

The first aim of this study was to compare the volume of thalamic nuclei between 22qdel carriers and a control group from childhood to adulthood, employing a longitudinal design. Then, we analyzed the role of AHs in the development of the thalamus and its nuclei. Finally, to exploit the relationship between structure and function, we computed whole-brain functional connectivity (FC) of nuclei showing an aberrant developmental trajectory in 22qdel carriers with AHs.

METHODS AND MATERIALS

Participants

In total, 120 subjects with a genetically confirmed diagnosis of 22q11DS and 110 healthy control subjects (HCs) were included in the current study, and their recruitment was carried on in the context of an ongoing longitudinal project investigating the brain development of 22qdel carriers (45). The subjects are followed up approximately every 3 years, and they undergo clinical and cognitive testing and the acquisition of neuroimaging data at each assessment. In this study, the inclusion criteria for the longitudinal analyses comprised the presence of a 3T scanner in good condition and Structured Interview for Psychosis–Risk Syndromes scores (46). In addition, we excluded from the current study 22qdel carriers with any other type of hallucination except AHs. The age of the patients and HCs ranged from 8 to 35 years, and the two groups were demographically matched (Table 1). For each participant, we included 1 to 4 scans (with an average of 1.94 visits per participant). Written informed consent was obtained from participants and/or their parents if minors. The study was approved by the cantonal ethics committee and was conducted according to the Declaration of Helsinki.

Psychiatric Assessment

Because the Structured Interview for Psychosis–Risk Syndromes has been shown to be a well-validated diagnostic tool for assessing psychotic symptoms in 22qdel carriers (41,42), it was administered to the patients at each visit by the same psychiatrist. To test our hypothesis on AHs, we looked at the P4 scale (i.e., the presence of hallucinations and perceptual abnormalities) with a focus on the module of auditory

Table 1. Demographic Information and Medical History Comprising Psychiatric Disorders and Medication Use in the Group of 22qdel Carriers and in the Subgroups With and Without Auditory Hallucinations

	HCs	All 22qdel Carriers	*p* Value	22qdel Carriers AH−	22qdel Carriers AH+	*p* Value
Number of Subjects, *n* (% Female)	110 (51.8%)	120 (57.1%)	.1072	64 (62.5%)	56 (53.57%)	.1033
Age, Years	17.40 ± 5.75	17.66 ± 5.95	.327	17.55 ± 5.73	18.07 ± 6.13	.0925
Age Range, Years	8–35	8–35	N/A	8–35	8–35	N/A
Total Number of Scans	210	232	N/A	112	120	N/A
Number of 3T (Trio) Scans	134	146	.1426	68	80	.1380
Number of 3T (Prisma) Scans	76	86	.1426	44	40	.1380
Subjects Medicated	0	68 (56.67%)	N/A	37 (57.81%)	31 (55.36%)	.2504
Methylphenidate	0	38 (31.67%)	N/A	22 (34.37%)	16 (28.57%)	.0647
Antidepressants	0	30 (25%)	N/A	14 (21.87%)	16 (28.57%)	.2348
Antipsychotics	0	15 (12.5%)	N/A	0	15 (23.44%)	<.001
Anxiolytics	0	17 (14.17%)	N/A	8 (12.5%)	9 (16.07%)	.2593
Antiepileptic drugs	0	7 (5.83%)	N/A	3 (4.68%)	4 (7.14%)	.2348
More than one class of medication	0	22 (18.33%)	N/A	12 (15.62%)	12 (21.43%)	.1064
Subjects Meeting Criteria for Psychiatric Diagnosis	0	77 (55%)	N/A	39 (60.94%)	38 (67.85%)	.2796
ADHD	0	49 (35%)	N/A	25 (39.06%)	24 (42.86%)	.2764
Generalized anxiety disorder	0	24 (17.14%)	N/A	15 (23.44%)	10 (17.86%)	.0573
Phobia	0	44 (31.43%)	N/A	24 (37.5%)	20 (35.71%)	.1635
Mood disorders	0	33 (23.57%)	N/A	15 (23.44%)	18 (32.14%)	.1998
Psychotic disorders	0	20 (14.28%)	N/A	0	20 (35.14%)	<.001
OCD	0	8 (5.71%)	N/A	4 (6.25%)	4 (7.14%)	.2850
More than one diagnosis	0	74 (52.86%)	N/A	36 (56.25%)	38 (67.85%)	.2639

Values are *n, n* (%), or mean ± SD.

ADHD, attention-deficit/hyperactivity disorder; AH+, with auditory hallucinations; AH−, without auditory hallucinations; HC, healthy control subject; N/A, not applicable; OCD, obsessive-compulsive disorder; 22qdel, 22q11.2 deletion.

distortions, illusions, and hallucinations. 22qdel carriers were categorized as having AHs if they had a score of 3 or higher on the P4 scale and positive answers in the module of auditory misperceptions or not having AHs when they had a score lower than 3 on the P4 scale. In addition, to disprove the contribution of other positive symptoms to the differences in thalamic nuclei volume and connectivity, we separately analyzed the P1, P2, P3, and P5 scales (delusional ideas, suspiciousness, grandiose ideas, and disorganized communication).

MRI Acquisition

T1-weighted scans were acquired with two different 3T scanners; a Siemens Trio was used for the first 280 scans and a Siemens Prisma was used for the remaining 162 scans (Siemens Corp., Erlangen, Germany) at the Center for Biomedical Imaging in Geneva, Switzerland. The proportion of scans with each MRI scanner did not differ between 22qdel carriers and HCs or between patients with and without AHs (Table 1). Nevertheless, the scan type was entered as a covariate in all the analyses in order to avoid confounding factors. Because longitudinal resting-state fMRI (rs-fMRI) data were not accessible for the vast majority of the subjects, we decided to perform a cross-sectional comparison of 22qdel carriers with and without AHs. The time point for cross-sectional analyses was selected according to the first emergence of AHs, and then we included an age-matched group of 22qdel carriers without AHs (Table S1). Good rs-fMRI data were available for 86 22qdel carriers, 42 with and 44 without AHs.

The parameters for the acquisition of structural images for the T1-weighted MPRAGE (magnetization prepared rapid acquisition gradient–echo) sequence were repetition time = 2500 ms, echo time = 3 ms, flip angle = 8°, acquisition matrix = 256 × 256, field of view = 23.5 cm, voxel size = 0.9 × 0.9 × 1.1 mm, and 192 slices. rs-fMRI data were recorded with a T2-weighted sequence of 8 minutes (voxel size = 1.84 × 1.84 × 3.2 mm, 38 slices, repetition time = 2400 ms, echo time = 30 ms, flip angle = 85°). During the resting-state session, participants were instructed to fixate a cross on the screen and not to fall asleep or let their mind wander.

Structural Images Pipeline

T1-weighted images underwent fully automated image processing with FreeSurfer version 6.0, comprising skull stripping, intensity normalization, reconstruction of internal and external cortical surfaces, and parcellation of subcortical brain regions (47).

Thalamic nuclei were labeled by using a probabilistic atlas of the thalamus based on Bayesian inference built combining histological delineation of 26 nuclei with in vivo manual segmentation of the thalamus and surrounding regions such as the hippocampus, putamen, and caudate (35). The names of the 26 nuclei of the thalamus provided by the segmentation are listed in Table 2. The quality of the segmentation was ensured by visual inspection, and 5 scans were excluded from further analyses (more details are provided in the Supplement).

Table 2. *p* Values and Log-Likelihood Ratio Values for Group Effect and Age × Group Interaction (Slope) of the Developmental Trajectories of 22qdel Carriers Compared With HCs (Left) and of 22qdel Carriers With Auditory Hallucinations Compared With Those Without Auditory Hallucinations (Right)

		22qdel Carriers vs. HCs				22qdel Carriers AH+ vs. 22qdel Carriers AH−			
		Group Effect		Slope		Group Effect		Slope	
Thalamic Nuclei	Region	*p* Value	Likelihood Ratio, *df*	*p* Value	Likelihood Ratio, *df*	*p* Value	Likelihood Ratio, *df*	*p* Value	Likelihood Ratio, *df*
MGN	Left	<.0001[a]	52.6, 2[a]	.6853	1.9, 1	.0021[a]	19.8, 2[a]	.0354[a]	9.5, 1[a]
	Right	<.0001[a]	35.1, 2[a]	.9343	0.1, 1	.0097[a]	12.2, 2[a]	.0249[a]	7.2, 1[a]
LGN	Left	<.0001[a]	25.7, 2[a]	.7539	1.2, 1	.0502	7.2, 2	.2646	2.5, 1
	Right	<.0001[a]	28.5, 2[a]	.9305	0.1, 1	.2234	3.3, 2	.6287	0.5, 1
PuI	Left	.0168[a]	10.5, 2[a]	.7304	1.7, 1	.1411	3.9, 2	.3859	0.7, 1
	Right	.0243[a]	9.7, 2[a]	.6199	4.9, 1	.0646	8.4, 2	.1949	5.9, 1
PuM	Left	<.0001[a]	28.1, 2[a]	.9824	0.1, 1	.0976	6.8, 2	.6840	0.3, 1
	Right	.0014[a]	16.1, 2[a]	.8191	0.3, 1	.0584	9.5, 2	.2468	3.9, 1
PuA	Left	.1310	5.8, 2	.8191	0.4, 1	.2334	3.5, 2	.9845	0.02, 1
	Right	.2901	3.6, 2	.7539	1.3, 1	.2234	3.5, 2	.6038	0.8, 1
PuL	Left	.5106	3.6, 2	.6853	1.2, 1	.6229	0.98, 2	.7974	0.15, 1
	Right	.3265	2.2, 2	.1391	2.2, 2	.1494	4.9, 2	.9925	0.08, 1
L-Sg	Left	.5427	2.1, 2	.7539	0.9, 1	.1031	6.6, 2	.8814	0.04, 1
	Right	.7606	0.9, 2	.7539	0.9, 1	.1040	6.3, 2	.5402	1.3, 1
MD	Left	.8381	0.6, 2	.9842	0.04, 1	.5446	1.3, 2	.4175	0.4, 1
	Right	.7515	1, 2	.8191	0.3, 1	.1448	5.1, 2	.6423	0.4, 1
Pf	Left	.8381	1.2, 2	.8191	1.2, 2	.2526	4.4, 2	.3383	2.1, 2
	Right	.1061	6.4, 2	.7539	1.3, 1	.1217	5.7, 2	.2856	3.2, 1
Pt	Left	.8381	0.9, 2	.9031	0.5, 1	.1448	5.2, 2	.6038	0.7, 1
	Right	.8381	0.6, 2	.8187	0.6, 1	.0794	8.7, 2	.2468	0.6, 1
Pc	Left	.0001[a]	18.2, 2[a]	.6853	1.9, 1	.2114	3.8, 2	.6039	0.8, 1
	Right	.0040[a]	14.4, 2[a]	.9351	0.05, 1	.0646	7.7, 2	.6113	3.8, 1
CM	Left	.5873	1.4, 2	.8191	0.04, 1	.2558	3.9	.7680	1.4, 1
	Right	.4160	1.7, 2	.4954	0.5, 1	.1217	5.7, 2	.3383	2.4, 1
CeM	Left	.3442	3.2, 2	.6853	2.8, 1	.0301[a]	11.5, 2[a]	.0610	7.1, 1
	Right	.1366	5.5, 2	.6199	4.9, 1	.1040	6.3, 2	.3743	2, 1
MV(Re)	Bilateral	.0025[a]	7.3, 2[a]	.0504	2.3, 1	.0262[a]	9.7, 2[a]	.0106[a]	10.9, 1[a]
CL	Left	.9154	4.5, 2	.9756	0.2, 1	.2114	3.8, 2	.5105	1.5, 1
	Right	.5427	5.4, 2	.8203	0.5, 1	.5535	1.3, 2	.6113	0.6, 1
VA	Left	.0361[a]	8.2, 2[a]	.7539	1.2, 1	.0302[a]	12, 2[a]	.0610	7.5, 1
	Right	<.0001[a]	25.2, 2[a]	.6199	3.8,1	.0719	8, 2	.1548	2, 1
VPL	Left	.8381	0.5, 2	.8191	0.2, 1	.1448	5, 2	.7477	1.1, 1
	Right	.5106	2.2, 2	.6853	2.2, 1	.0806	5.1, 2	.5219	0.2, 1
VLa	Left	.0151[a]	10.8, 2[a]	.8191	0.4, 1	.2114	3.9, 2	.3383	2.7, 1
	Right	.0002[a]	17.3, 2[a]	.5847	0.3, 1	.0852	7.2, 2	.3383	2.5, 1
VLp	Left	.1366	5.4, 2	.9824	0.02, 1	.1811	3.4, 2	.4364	0.6, 1
	Right	.1366	7.2, 2	.8191	1.4, 1	.0852	7.4, 2	.3383	2.4, 1
VM	Left	.3405	3.2, 2	.9824	0.04, 1	.2234	3.3, 2	.5529	1.1, 1
	Right	.2901	5.3, 2	.9351	0.05, 1	.2114	3.8, 2	.6113	0.6, 1
AV	Left	.6580	1.4, 2	.9824	0.03, 1	.0300[a]	11.9, 2[a]	.2468	4.2, 1
	Right	.2901	3.7, 2	.6853	2.01, 1	.2123	3.7, 2	.6113	0.5, 1
LP	Left	<.0001[a]	23.4, 2[a]	.6199	4.3, 1	.0380[a]	11.2, 2[a]	.2066	4.9, 1
	Right	<.0001[a]	29.6, 2[a]	.7539	1.2, 1	.1535	4.7, 2	.5529	1.2, 1
LD	Left	.6838	1.3, 2	.8191	0.3, 1	.2234	3.3, 2	.8814	0.04, 1
	Right	.8417	0.4, 2	.9351	0.06, 1	.7971	0.5, 2	.8424	0.09, 1

Table 2. Continued

Thalamic Nuclei	Region	22qdel Carriers vs. HCs				22qdel Carriers AH+ vs. 22qdel Carriers AH−			
		Group Effect		Slope		Group Effect		Slope	
		p Value	Likelihood Ratio, *df*	*p* Value	Likelihood Ratio, *df*	*p* Value	Likelihood Ratio, *df*	*p* Value	Likelihood Ratio, *df*
Thalamus	Left	.8296	0.7, 2	.8189	0.2, 2	.1037	6.5, 1	.8814	0.04, 1
	Right	.8417	0.4, 2	.8191	0.4, 1	.0746	8.5, 2	.5402	1.3, 1

All the *p* values are corrected for multiple comparisons.

AV, anteroventral; CeM, central medial; CL, central lateral; CM, centromedian; HC, healthy control subject; LD, laterodorsal; LGN, lateral geniculate nucleus; LP, lateral posterior; L-Sg, limitans suprageniculate; MD, mediodorsal nucleus; MGN, medial geniculate nucleus; MV(Re), reuniens (medial ventral); Pc, paracentral; Pf, parafascicular; Pt, paratenial; PuA, anterior pulvinar; PuI, inferior putamen; PuL, lateral pulvinar; PuM, medial pulvinar; 22qdel, 22q11.2 deletion; VA, ventral anterior; Vamc, ventral anterior magnocellular; VLa, ventral lateral anterior; VLp, ventral lateral posterior; VM, ventromedial; VPL, ventral posterolateral.

[a]$p < .05$.

Estimation of the Developmental Trajectories

Owing to the characteristics of our sample, comprising a number of visits ranging from 1 to 4 with a variable time interval and an inconstant age distribution across the visits, we used a mixed-model regression analysis described in previous studies (45,48). Age and diagnosis were modeled as fixed effects, and within-subject factors were modeled as random effects with the function nlmefit in MATLAB R2017a (The MathWorks, Inc., Natick, MA). Total intracranial volume, sex, scanner model, and lifetime use of antipsychotic medications were entered into the model as covariates. Random-slope models (from constant to cubic) were fitted to the data, taking into account within-subject and between-subject effects. The most suitable model order was then selected using the Bayesian information criterion, and results were finally corrected for multiple comparisons with false discovery rate correction. Further details are provided in the Supplement.

Functional Images Pipeline

Functional images were preprocessed using SPM12, the Conn fMRI functional connectivity toolbox version 18 (49), and ART (Artifact Detection Tools) (50) for a rigorous control of head motion. Bilateral labels of each thalamic nucleus with aberrant development in subjects having AHs were used as seeds, and seed-to-voxel and region of interest (ROI)-to-ROI FC analyses were carried out with Conn. A comprehensive explanation of rs-fMRI image preprocessing and analyses is provided in the Supplement.

RESULTS

Developmental Trajectories of Thalamic Nuclei in 22qdel Carriers Compared With HCs

Model selection based on the Bayesian information criterion resulted in a first-order model for all thalamic nuclei, meaning that the relationship between age and volume was linear. All statistical values for the group effect and the interaction with age are listed in Table 2; the percentages of volume reduction or increase between groups are compared in Tables S2–S4, where further statistics regarding laterality and the type of scanner are also available.

Neither the average volume of the whole thalamus nor its developmental trajectory differed between 22qdel carriers and HCs. Instead, two ensembles of thalamic nuclei displayed either a higher or lower volume in the group of patients with respect to HCs. Thalamic nuclei involved in sensory relay, such as the MGN and lateral geniculate nucleus, and in sensory and attentional processing, such as the pulvinar and lateral posterior (LP) nuclei, were on average bilaterally smaller as compared with the control group (Figure 1). We did not find statistically significant differences between the developmental trajectories of these nuclei.

On the other hand, the paracentral (Pc) nucleus and an ensemble of anterolateral nuclei (ventrolateral anterior and ventral anterior [VA]) resulted in having a bigger volume in 22qdel carriers with respect to HCs. The right VA and left Pc nuclei showed a faster volume decrease in the group of control subjects, but these results did not survive false discovery rate correction. The nucleus medioventral reuniens showed a different developmental trajectory in 22qdel carriers as compared with HCs (Figure 2).

Developmental Trajectories of Thalamic Nuclei in Relation to AHs

Different positive psychotic symptoms as measured by the Structured Interview for Psychosis–Risk Syndromes comprising hallucinations, delusions, suspiciousness, and disorganization were used to divide 22qdel carriers into two groups with high and low scores of symptoms. It was not possible to use grandiose ideas to dichotomize patients because fewer than 5 subjects experienced these symptoms.

When considering positive symptoms other than AHs, we did not find any significant differences after correcting for multiple comparisons (Table S5). Conversely, 22qdel carriers with AHs had a smaller volume of MGN bilaterally with a steeper volume decrease with respect to 22qdel carriers without AHs. This divergence in the trajectories of MGN volume started early in development, at around 10 years for the right MGN and before 8 years for the left MGN (Figure 3).

Patients with AHs also showed a deviant developmental trajectory of left-side nuclei involved in higher cognitive functions, characterized by a lower volume followed by an increase of volume with respect to 22qdel carriers without AHs, that started at different ages (medioventral reuniens: 17.2 years; central medial: 20.4 years; VA: 21.2 years; LP: 24.6 years; anteroventral (AV): 26.9 years). The developmental effect

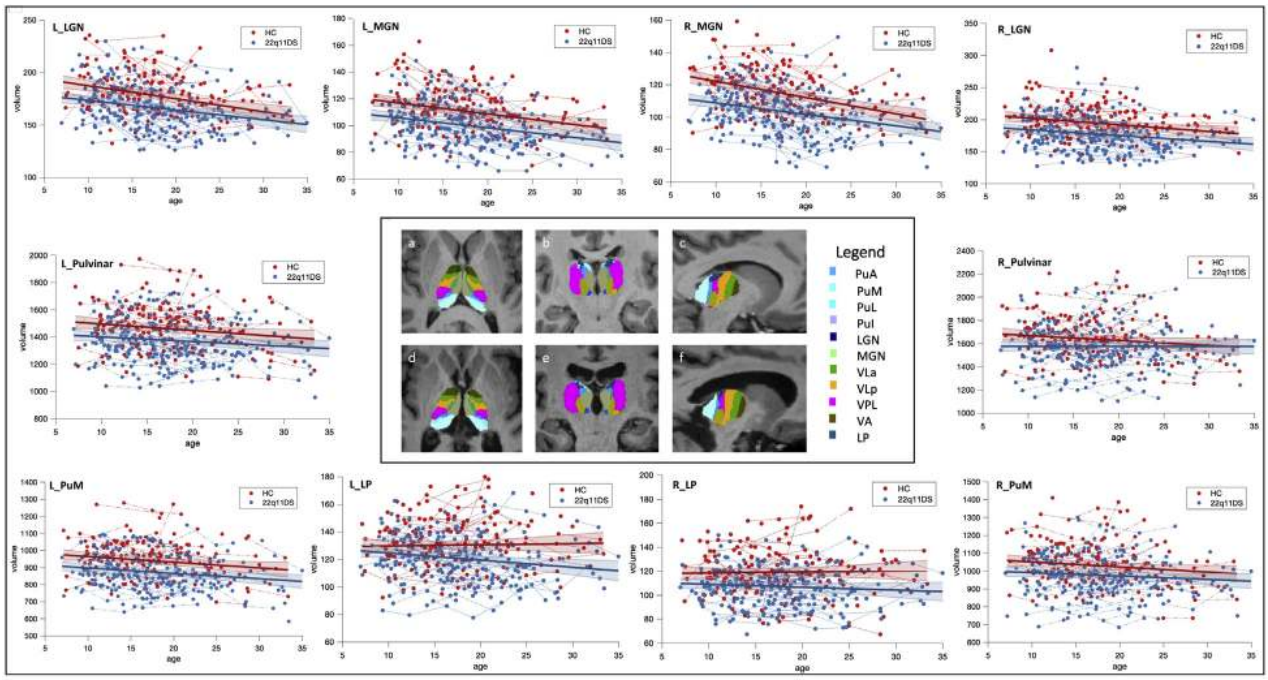

Figure 1. Comparison between patients with 22q11.2 deletion syndrome (22q11DS; in blue) and healthy control subjects (HC; in red). Mixed-model analysis of the developmental trajectories shows a marked smaller volume of the medial geniculate nucleus (MGN), lateral geniculate nucleus (LGN), pulvinar, and lateral posterior nucleus (LP) in patients with 22q11DS. Central panel: Example of thalamic segmentation in a deletion carrier (lower figures) and one healthy control (upper figures) showing the nuclei of interest in axial (a, d), coronal (b, e) and sagittal (c, f) sections. Volumes are expressed in mm^3. L, left; PuA, anterior pulvinar; PuI, inferior putamen; PuL, lateral pulvinar; PuM, medial pulvinar; R, right; VA, ventral anterior; VLa, ventral lateral anterior; VLp, ventral lateral posterior; VPL, ventral posterolateral.

survived correction for multiple testing only for the nucleus medioventral-reuniens (MV-Re) and bilateral MGN.

FC of Thalamic Nuclei With Aberrant Development in Patients With AHs

To investigate whether the structural abnormalities had a functional correlate, we performed seed-to-voxel and ROI-to-ROI resting-state FC analyses of each thalamic nucleus with an aberrant development in 22qdel carriers with AHs. fMRI motion parameters and the standard deviation of the signal did not differ between 22qdel carriers with and without AHs (Table S6). Average measures of the left/right ROI volumes with standard deviations were 114.8 ± 20.3/126.9 ± 22.3 mm^3 for the AV, 420.9 ± 55.5/431.5 ± 53.2 mm^3 for the VA, 119.6 ± 17.5/106.2 ± 16.1 mm^3 for the LP, 102.6 ± 14.7/99.8 ± 15.6 mm^3 for the MGN, 55.95 ± 8.4/61.2 ± 8.4 mm^3 for the central medial, and 19 ± 3.6 for the MV-Re. We decided to exclude MV-Re and central medial nuclei from the analysis because their volume was too small to give reliable results (<5 voxels). Seed-to-voxel analyses did not yield a significant difference for any nucleus of the thalamus; however, when employing a ROI-to-ROI approach, we found a statistically significant pattern of increased thalamocortical FC of the MGN and AV nuclei with primary and associative temporo-occipital regions implied in auditory processing and speech comprehension (Tables 3 and 4 and Figures 4 and 5). Thalamocortical connectivity values for each nucleus in each group and group differences of FC are available in Figures S1 to S3 and Tables S7 and S8.

To test our hypothesis that the aberrant development of gray matter was implied in the dysconnectivity of the MGN with temporo-occipital cortical regions, the values of FC were finally correlated with the volumes of the left and right MGN. A negative correlation of the FC between the left MGN and anterior superior temporal gyrus with the volume of the left MGN ($r = -.375$, $p = .002$) was significant (Figure 5).

DISCUSSION

Individuals With 22q11DS Have a Selective Impairment of the Thalamus

Despite exhibiting either a lower or higher volume of distinct thalamic nuclei, 22qdel carriers did not show any difference in the overall volume of the thalamus as compared with HCs. Regarding subjects at clinical and genetic risk for psychosis, the current literature shows mixed findings. While there is strong meta-analytic evidence for thalamic volume reduction in patients with schizophrenia, when analyzing earlier phases of the disease the results are more variable (1,27). Individuals at their first episode of psychosis have a selective lower volume of midline thalamic nuclei (29) and microstructural damage of the mediodorsal nucleus and pulvinar (51), while siblings of patients with schizophrenia were found to have lower volumes of the anterior thalamus (52). Altogether, these results are highly heterogeneous on both temporal and spatial scales. To

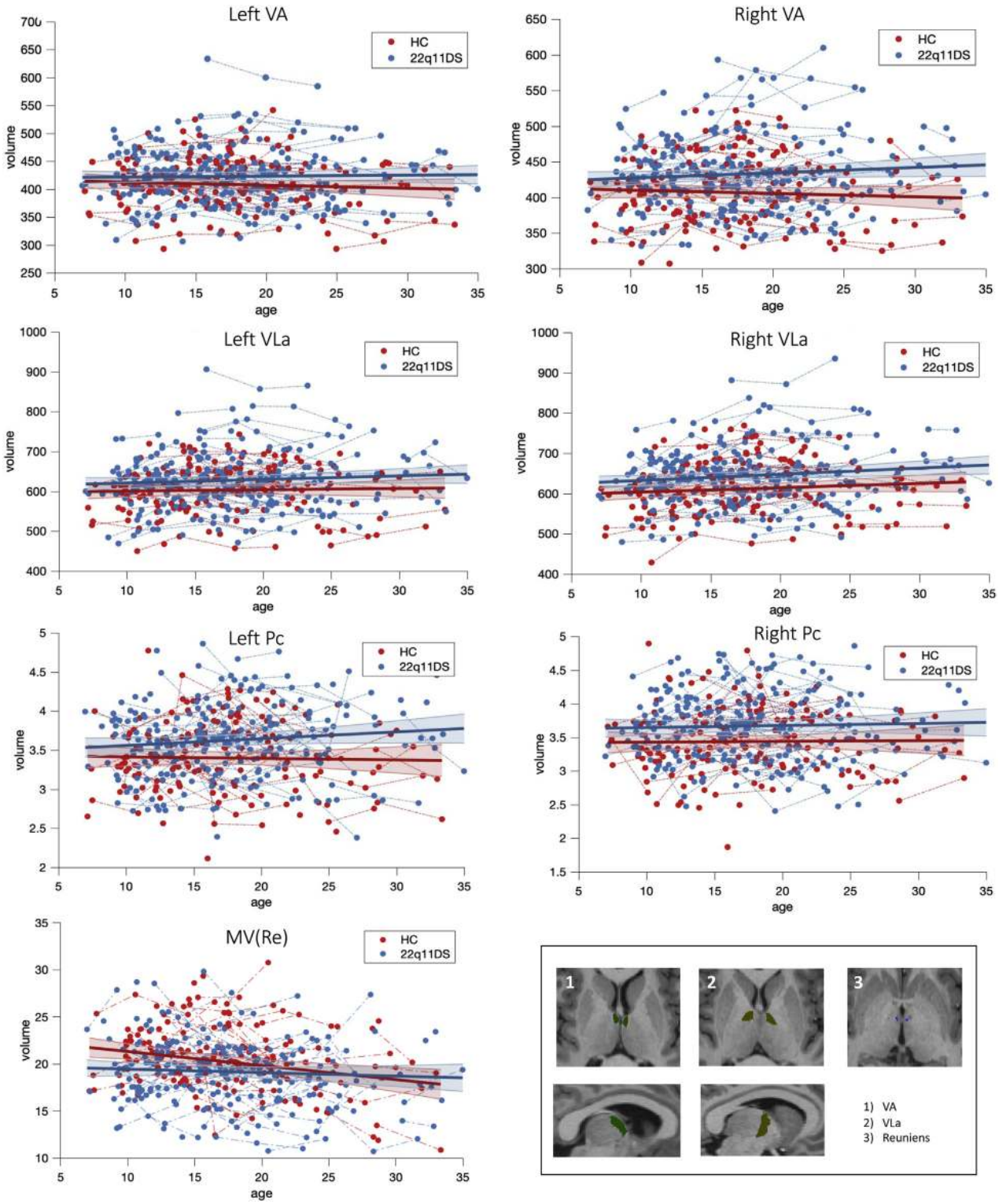

Figure 2. Comparison between patients with 22q11.2 deletion syndrome (22q11DS; in blue) and healthy control subjects (HC; in red). Mixed-model analysis of the developmental trajectories shows a higher volume of the ventral-anterior nucleus (VA), ventrolateral anterior nucleus (VLa), paracentral nucleus (Pc), and nucleus medioventral reuniens [MV(Re)] in patients with 22q11DS. Lower panel: Example of thalamic segmentation showing the nuclei of interest in coronal and sagittal sections. Volumes are expressed in mm^3.

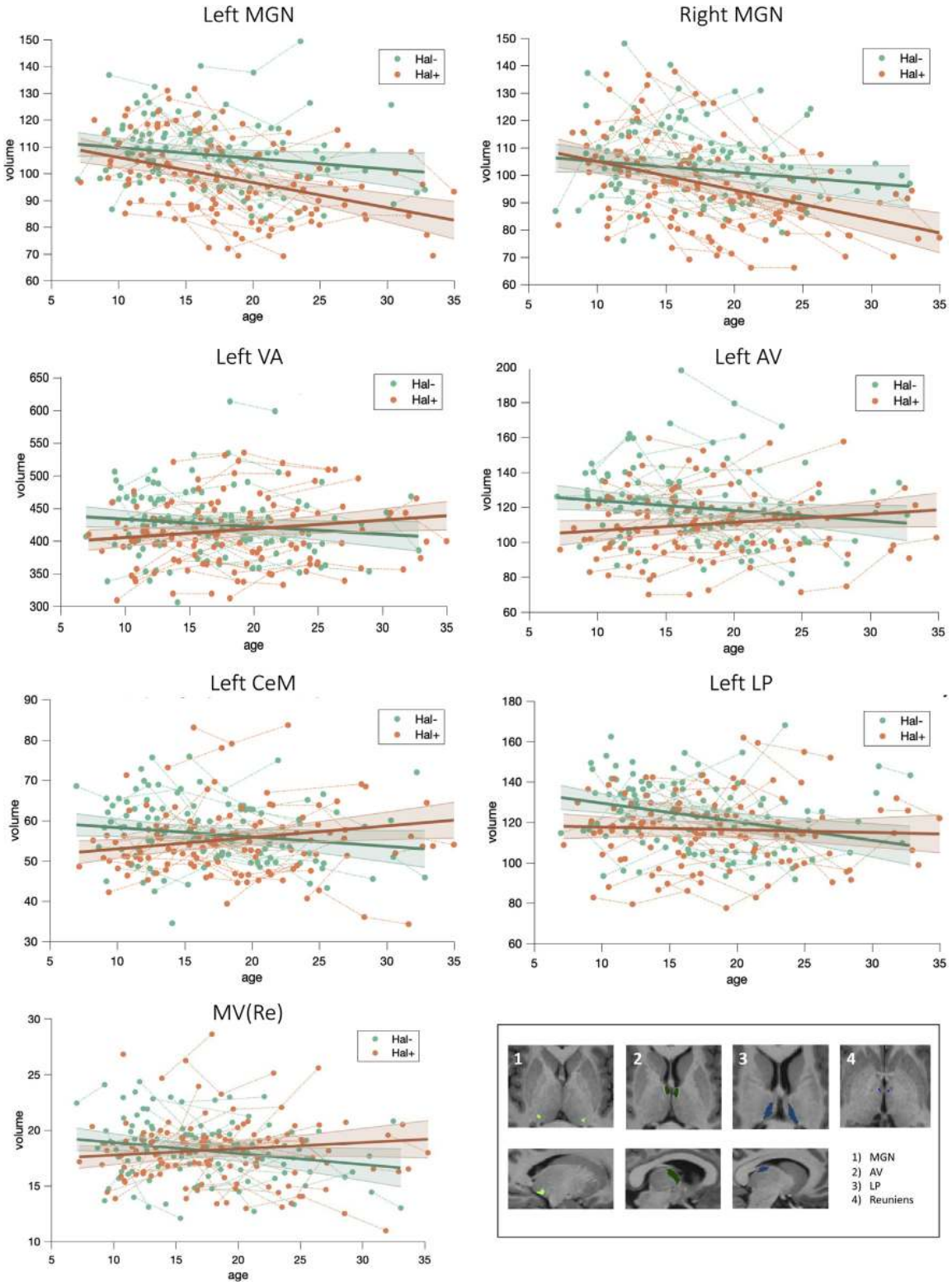

Figure 3. Comparison between patients with 22q11.2 deletion syndrome with auditory hallucinations (AHs) (Hal+; in orange) and without AHs (Hal−; in green). Upper plots: Mixed-model analysis of the developmental trajectories showing a smaller volume of the bilateral medial geniculate nucleus (MGN) and an interaction with age in patients with AHs. The other plots show deviant developmental trajectories of left-side nuclei comprising the ventral anterior (VA), anteroventral (AV), central medial (CeM), lateral posterior (LP), and nucleus medioventral reuniens [MV(Re)] bilaterally in patients with AHs. Lower panel: Example of thalamic segmentation showing the nuclei of interest in coronal and sagittal sections. Volumes are expressed in mm^3.

Table 3. Group Differences (AH+ > AH−) in ROI-to-ROI Functional Connectivity Between the Left and Right MGN and the Whole Brain Using Harvard–Oxford Atlas

	Left MGN			Right MGN		
	t Value	*p* Value	*p* Value FDR	*t* Value	*p* Value	*p* Value FDR
Right TP	3.70	.0002	.0217[a]	3.38	.0006	.0471[a]
Left DMN.LP	3.59	.0003	.0217[a]	2.86	.0028	.0637
Left TOFusC	3.49	.0004	.0217[a]	2.93	.0023	.0637
Left sLOC	3.42	.0005	.0217[a]	2.76	.0037	.0637
Left PT	3.35	.0007	.0218[a]	3.28	.0008	.0471[a]
Left aSTG	3.16	.0012	.0286[a]	3.27	.0008	.0471[a]
Right TOFusc	3.15	.0012	.0286[a]	2.79	.0034	.0637

Only statistically significant results are reported.

AH+, with auditory hallucinations; AH−, without auditory hallucinations; aSTG, anterior superior temporal gyrus; DMN.LP, default mode network, seed lateral parietal cortex; FDR, false discovery rate; MGN, medial geniculate nucleus; PT, planum temporale; ROI, region of interest; sLOC, lateral occipital cortex; TOFusC, temporo-occipital fusiform cortex; TP, temporal pole.

[a]$p < .05$.

our knowledge, only one study has investigated the volume of the thalamus in children with 22q11DS, highlighting a selective reduction of the posterior thalamus (53). Owing to the lack of advanced segmentation techniques at the time, this volume decline was entirely attributed to the pulvinar (53). However, it is likely that the lower volume of other posterior thalamic nuclei contributed to that finding.

Indeed, in our study, the volume of posterior thalamic nuclei involved in sensory processing was lower in 22qdel carriers. The lateral geniculate nucleus and MGN are the principal relay nuclei for visual and auditory pathways, respectively, and it is well known that 22qdel carriers have extensive impairments in sensory domains (54). Neural responses to auditory stimulation are decreased in 22qdel carriers and, similar to patients with schizophrenia, they have inefficient mechanisms of sensory gating (55–57). Moreover, specific impairments in visuospatial skills have been related to the syndrome (58,59). The pulvinar and LP nuclei cooperate to determine visual saliency and to allocate attentional resources during visual processing by synchronizing the activity across visual cortices (60,61). It has been consistently shown that 22qdel carriers have selective deficits in executive visual attention (62,63). Furthermore, the lower volume of the pulvinar was mostly driven by a volumetric reduction of the medial pulvinar, a subregion with extensive and reciprocal connectivity with higher-order cortices involved in the simultaneous processing of multimodal stimuli (64). The volume of the medial pulvinar is reduced in patients with schizophrenia and has been implicated in the genesis of symptoms such as impaired attentional performance and abnormal vision-guided behavior (65).

Our findings also highlighted the presence of thalamic nuclei with a bigger volume in 22qdel carriers as compared with HCs. Specifically, VA and ventrolateral nuclei are intercalated in a circuit comprising the basal ganglia, cerebellum, and premotor cortex, aimed at motor planning. To date, a variety of movement disorders has been reported in 22qdel carriers (66,67). However, it is not clear whether this psychomotor phenotype pertains to a more general predisposition of the syndrome to multiple motor abnormalities or to specific disturbances such as catatonic schizophrenia, parkinsonism,

Table 4. Group Differences (AH+ > AH−) in ROI-to-ROI Functional Connectivity Between the Left and Right AV Nucleus and the Whole Brain Using Harvard–Oxford Atlas

	Left AV Nucleus			Right AV Nucleus		
	t Value	*p* Value	*p* Value FDR	*t* Value	*p* Value	*p* Value FDR
Left pSMG	3.66	.0005	.0307[a]	3.61	.00057	.0382[a]
Left FOrb	3.65	.0005	.0307[a]	3.43	.0010	.0382[a]
Left aSTG	3.59	.0006	.0307[a]	3.42	.0011	.0382[a]
Left sLOC	3.51	.0008	.0307[a]	3.41	.0012	.0382[a]
Left PT	3.46	.0009	.0307[a]	3.53	.0007	.0382[a]
Left AG	3.42	.0010	.0307[a]	3.16	.0023	.0502
Left Language.pSTG	3.31	.0015	.0336[a]	3.18	.0022	.0502
Right TP	3.29	.0016	.0336[a]	2.98	.0040	.0649
Left DMN.LP	3.26	.0017	.0336[a]	3.03	.0034	.0649
Right PT	3.04	.0034	.0586	3.18	.0022	.0502

Only statistically significant results are reported.

AG, angular gyrus; AH+, with auditory hallucinations; AH−, without auditory hallucinations; aSTG, anterior superior temporal gyrus; AV, anteroventral; DMN.LP, default mode network, seed lateral parietal cortex; FDR, false discovery rate; FOrb, orbitofrontal cortex; Left Language.pSTG, language network, seed posterior superior temporal gyrus; pSMG, posterior supramarginal gyrus; PT, planum temporale; ROI, region of interest; sLOC, lateral occipital cortex; TP, temporal pole.

[a]$p < .05$.

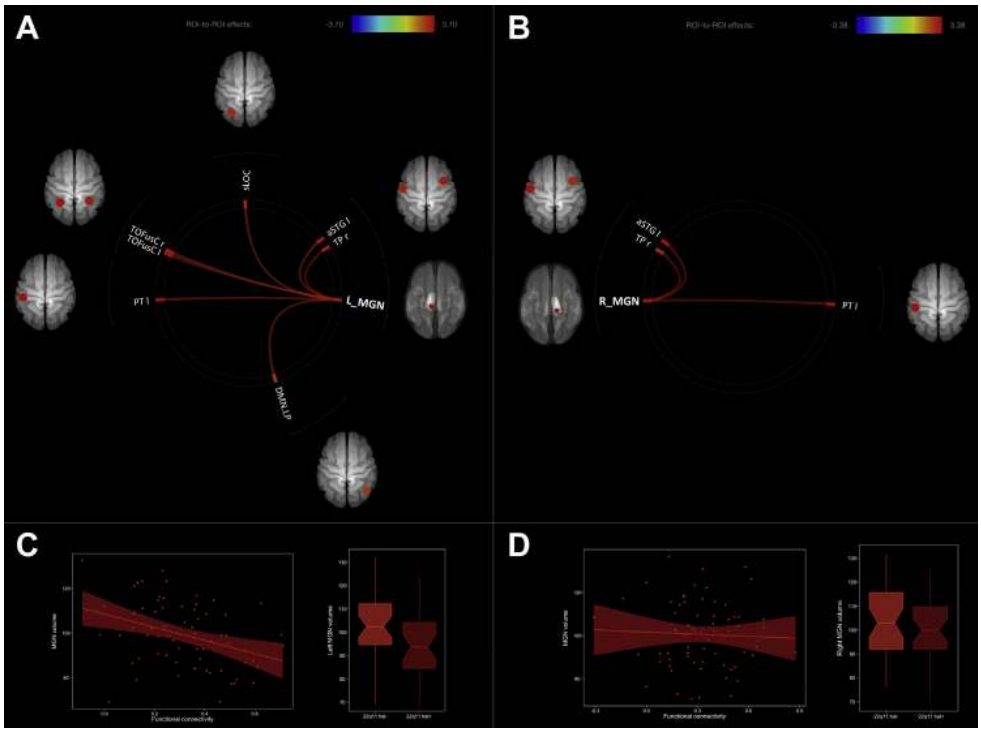

Figure 4. Functional connectivity (FC) of the medial geniculate nucleus (MGN). **(A, B)** FC of the left and right MGN with cortical regions. Only regions of interest (ROIs) with a statistically significant increased FC with MGN in patients with 22q11.2 deletion syndrome (22qdel carriers) with auditory hallucinations are shown. *t* Values of ROI-to-ROI FC are expressed with a color code displayed in the figure. **(C)** Correlation between left MGN volume and values of FC between the left MGN and the left anterior superior temporal gyrus (aSTG l) on the left and boxplots of left MGN volume in 22qdel carriers with and without auditory hallucinations (hal+ and hal−, respectively). **(D)** Same description as **(C)** but for the right MGN. DMN.LP, default mode network, seed lateral parietal cortex; L, left; PT l, left planum temporale; R, right; sLOC, lateral occipital cortex; TOFusC l, left temporo-occipital fusiform cortex; TOFusC r, right temporo-occipital fusiform cortex; TP r, right temporal pole.

and endocrine diseases. Another nucleus exhibiting a bigger volume in 22qdel carriers was the Pc, one of the intralaminar nuclei reciprocally connected with a broad set of cortical and subcortical regions (68). Interestingly, the Pc is supposed to have a role in so-called cognitive awareness, given that lesions in this nucleus lead to the dysexecutive syndrome that well aligns with executive function disturbances in 22qdel carriers (69).

Overall, 22qdel carriers were found to have a pattern of decreased volume in sensory nuclei and increased volume in some of the nuclei involved in higher cognitive functions and motor planning, with a developmental trajectory parallel to that of HCs, suggesting an early occurrence of these abnormalities. Translational studies demonstrated that the development of thalamic nuclei is already defined in utero and is finely orchestrated by a set of genes coding for transcription factors (70,71). Although none of the genes known to guide the differentiation of the thalamus is located within the 22q11.2 region, possibly cross-genes interaction led by regulatory genes (72) might account for the early abnormalities of thalamic nuclei in 22qdel carriers.

AHs Are Related to Abnormal Development of Distinct Thalamic Nuclei

In agreement with the literature on psychosis, the most affected thalamic nuclei in 22qdel carriers experiencing AHs pertained to the domains of working memory and auditory stimuli processing, suggesting a causal nexus. Concerning nuclei involved in cognitive functions, we found a lateralized involvement on the left side, consistent with previous studies (30,32,52,73). As we hypothesized, MGN volume was bilaterally lower in the group with AHs and the extent of the volume loss increased over time. Even in HCs, there was a propensity to a linear volume decrease; however, in patients with AHs, the atrophy rate was accentuated and the developmental trajectory diverged from that of 22qdel carriers without AHs during childhood. Therefore, the maturation of MGN in those subjects who will experience AHs is aberrant throughout a wide period spanning from late childhood to adulthood.

On the other hand, the only other nucleus with a significant deviant development was the nucleus medioventral reuniens; in subjects with AHs, we found a substantially divergent trajectory with the point of inflection during late adolescence. Interestingly, the MV-Re facilitates the communication between the prefrontal cortex and hippocampus during memory processes (74,75) and has been proposed as a central hub of a thalamo–hippocampal–ventral tegmental area loop that possibly underlies psychotic symptoms (Figure 6). According to this theory, a primary NMDA receptor hypofunction disinhibiting the MV-Re would lead to a hyperactivation of the hippocampus and consequently an aberrant activation of the dopamine system with heightened dopamine release in the thalamus and thereby a positive feedback loop (76). In line with this theory, we found a sharp volume drop of the hippocampus during late adolescence, starting from the CA1 subfield in a largely overlapping sample of 22qdel carriers with psychotic symptoms (45), and our data seem to confirm the existence of a correlation between CA1 and MV-Re volume (Table S11). Remarkably, the MV-Re and CA1 are reciprocally connected, and therefore their divergent developmental trajectories during

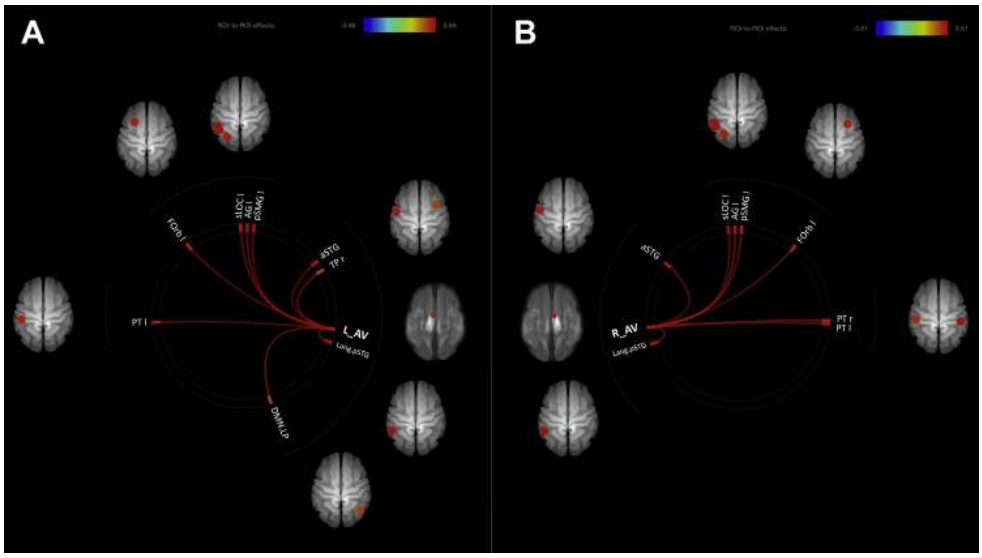

Figure 5. Functional connectivity (FC) of the anteroventral (AV) nucleus. FC of the left AV nucleus **(A)** and right AV nucleus **(B)** with cortical regions is shown. Only regions of interest (ROIs) with a statistically significant increased FC with AV in patients with 22q11.2 deletion syndrome with auditory hallucinations are shown in the figure. *t* Values of ROI-to-ROI FC are expressed with a color code displayed in the figure. AG l, left angular gyrus; aSTG, anterior superior temporal gyrus; FOrb l, left orbitofrontal cortex; L. left; Lang.pSTG, language network, seed posterior superior temporal gyrus; pSMG l, left posterior supramarginal gyrus; PT l, left planum temporale; PT r, right planum temporale; R, right; sLOC l, left lateral occipital cortex; TP r, right temporal pole.

late adolescence might account for the emergence of this positive loop concomitantly with the onset of positive psychotic symptoms. In line with this hypothesis, early abnormalities of CA1 that can be rescued only during a critical time window comprising late adolescence have been reported in mouse models of 22q11DS (77).

Of all the nuclei with a different volume in 22qdel carriers with AHs, only the AV did not differ in the comparison between HCs and the whole group of individuals with 22q11DS. The AV nucleus contributes to reciprocal hippocampal–prefrontal interactions and has been suggested to have a crucial role in promoting synaptic plasticity in the

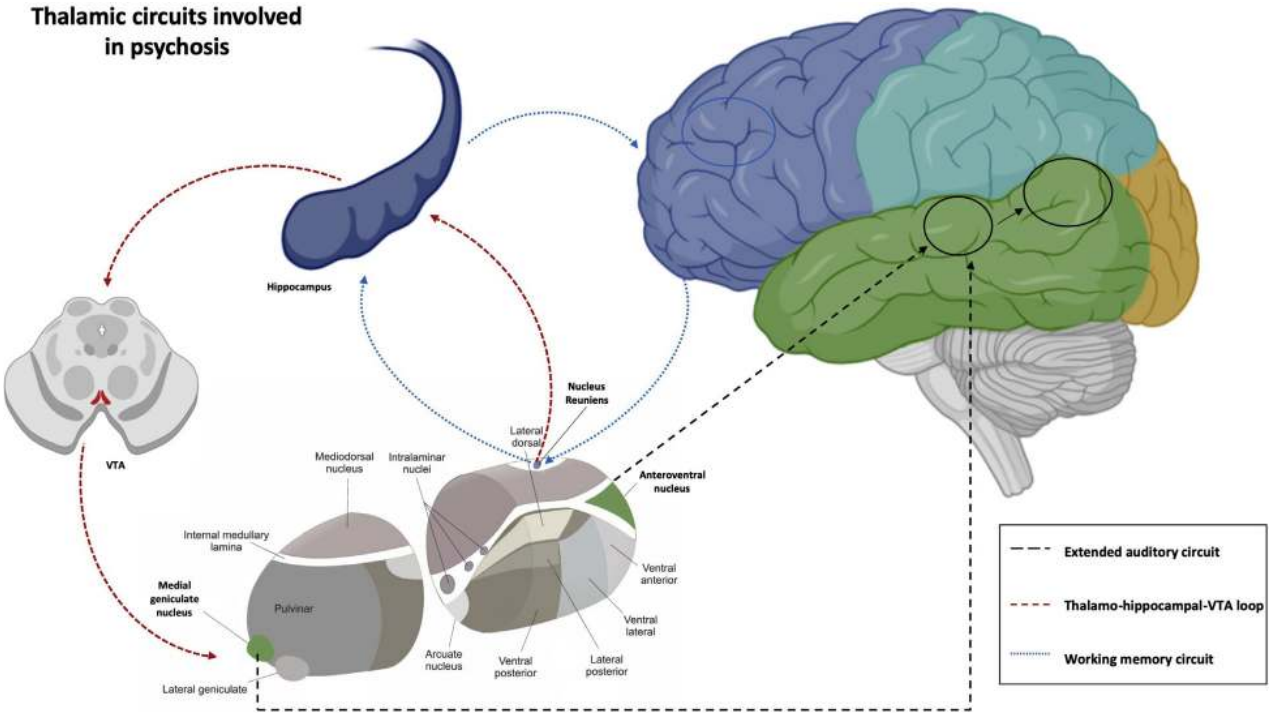

Figure 6. Thalamic circuits possibly involved in psychosis in patients with 22q11.2 deletion syndrome. Extended auditory circuit: increased connectivity from the medial geniculate nucleus and anteroventral nucleus to the auditory cortex and Wernicke's area. Thalamo–hippocampal–ventral tegmental area (VTA) loop: positive feedback circuit that has been proposed to underlie the onset of psychotic symptoms starting from a dysfunction of the nucleus medioventral reuniens. Working memory circuit: where the dorsolateral prefrontal cortex can communicate with the hippocampus only through the nucleus medioventral reuniens.

hippocampus to such an extent that its lesion may cause episodic memory deficits (5,78). A lower volume of the anterior thalamus is one of the most replicated findings within the psychosis continuum, from subjects at clinical or genetic risk for schizophrenia to patients with chronic disease (1–3,52), and memory deficits are now considered as part of the core symptoms of schizophrenia.

When other positive symptoms of psychosis were taken into account, no correlation with the volume or development of thalamic nuclei was observed. Consequently, it is possible that aberrant thalamocortical structure development is selectively implied in the pathophysiology of AHs but is partially independent from brain dynamics underlying other psychotic symptoms.

Deletion Carriers With AHs Have an Immature Pattern of Thalamocortical Connectivity

The 22qdel carriers experiencing AHs have an increased thalamocortical connectivity from the MGN to the left AC and associative areas within Wernicke's area (79). Remarkably, the strong left cortical lateralization, rather than being related to differences in the proportion of left-handedness in the two groups, most likely reflects the involvement of language-associated brain areas. Indeed, the hyperactivity of language-related regions has been mechanistically implied in the origin of auditory verbal hallucinations (14,22,80) as well as increased thalamic connectivity with the AC (23). More broadly, a pattern of thalamocortical dysconnectivity with sensory regions has been consistently reported as a hallmark of psychosis (33,81) and has been previously revealed in 22qdel carriers (82). Our findings point toward a specific involvement of regions intercalated in the auditory pathway and language network in 22qdel carriers at their first experience of AHs. In other words, we showed that the MGN is hyperconnected not only to the AC but also to speech processing areas, providing a conceptual framework for the emergence of AHs in 22qdel carriers.

Interestingly, an fMRI study during an auditory task based on monitoring self-generated speech highlighted the hypoactivation of the MGN in patients with schizophrenia and poor performance (83). Taken together with our findings, the MGN seems to be hypoactive during speech tasks but hyperconnected to the AC and brain areas involved in language perception during rest. This is in line with the concept of paradoxical activation proposed by Kompus *et al.* and corroborated by the multimodal findings of increased neural activity at rest and disengagement during task of the AC in patients with AHs (9,84). The left AC was the area with the highest paradoxical activation by means of an intersection analysis of many studies (9). We further propose that such a pattern might be mediated by either an increased or decreased recruitment of the AC by the MGN. Moreover, in our sample, we also demonstrated that the left MGN was hyperconnected to the default mode network (DMN), a network implied in self-referential processing that is activated at rest but disengaged during the execution of externally directed cognitive tasks (85,86). In patients with idiopathic schizophrenia as well as in 22qdel carriers, several studies have identified a failure to deactivate the DMN during active task and a decreased within-network and increased between-network connectivity at rest (87–94). Hence, it has been hypothesized that abnormal activity in the DMN might contribute to the generation of AHs by activating the AC at rest (95,96). Our data suggested that the aforementioned recruitment of the auditory system may occur even lower in the auditory hierarchy at the level of the sensory thalamus. Overall, abnormalities primarily attributed to the AC in subjects experiencing AHs may be a consequence of aberrant thalamocortical connectivity to the AC.

When looking at the connectivity of LP, VA and AV nuclei, only the latter exhibited a different pattern of thalamocortical connectivity in subjects with AHs. Strikingly, we found an increased FC with the AC, Wernicke's area, DMN, and language network. While the interpretation of the hyperconnectivity of the MGN with the AC and Wernicke's area is straightforward, the AV nucleus is not anatomically connected to these regions in a direct way. However, rs-fMRI is more likely to represent polysynaptic connectivity than monosynaptic connectivity (97,98). Moreover, the contribution of recent studies to the development of thalamocortical connectivity in the general population may shed light on our findings. Indeed, thalamocortical FC undergoes profound refinement from childhood to adulthood, including a weakening of connectivity with the AC and a transition from a widespread pattern to a localized pattern of projections from the thalamus (99). During childhood and puberty, anterior and midline thalamic nuclei are projecting to the temporal cortex; however, during adulthood, only a posterior region of the thalamus corresponding to the MGN is connected to the temporal cortex, and the strength of such connectivity is less than that in children (99). Therefore, considering that the mean age of 22qdel carriers experiencing AHs is shifted toward early adulthood, we can speculate that the emergence of AHs might be favored by an immature pattern of thalamocortical connectivity with the AC. Another explanation is that our findings could reflect an abnormally increased axonal branching related to genes located within the 22q11.2 region such as the *NGR1* gene (100,101).

A Developmental Framework for Thalamic Abnormalities

Altogether, our results point to an aberrant development of the thalamic nuclei that are hyperconnected to the AC and speech-related brain areas. Moreover, we found the distinct results of deviant developmental trajectories of left MGN volume and the immature pattern of its connectivity with the AC to be inversely correlated; that is, the smaller the MGN volume, the higher its connectivity to the AC. A negative correlation between thalamic volume and its increased connectivity has consistently been reported in a sample of individuals at clinical high risk for psychosis (24). Where interactions between the thalamus and cortex are concerned, an increased level of complexity is brought by the reciprocal influence on the development of each structure. Indeed, thalamocortical axons are known to finely shape the organization of primary sensory cortices, and the altered size of thalamic nuclei can influence the size of their cortical targets and lead to ectopic innervation of cortical regions from other unrelated thalamic nuclei (71). Interestingly, cortical areas targeted by the MGN and AV in our study—such as the AC—undergo a remarkable volume loss in patients with idiopathic schizophrenia and 22qdel carriers experiencing AHs (102–104). Overall, an early accelerated

volume decrease of the MGN may put in place a series of regulatory mechanisms that determine both the aberrant comaturation of target cortical regions and an immature pattern of connectivity that can favor the emergence of AHs by recruiting the AC at rest.

Limitations and Conclusions

Several limitations need to be highlighted. First, the segmentation technique employed in the current study is based on a probabilistic atlas constructed from MRI of adults and showed different rates of test–retest reliability depending on the nucleus. Therefore, we ensured that the magnitude of volumetric differences between the groups tested was higher than the margin of error of the test–retest reliability of the segmentation technique (Table S2). However, because the values for test–retest reliability were available for only some of the thalamic nuclei (35), our results need replication.

Second, two types of scanner were used during the longitudinal study; however, we covaried all the analyses for the type of scanner, and the proportion of scans acquired with each scanner did not differ between the groups. Similarly, we ensured that all the possible confounds such as demographic characteristics, psychiatric comorbidities, and medication intake, as well as motion parameters, deafness, and laterality in the case of rs-fMRI, did not differ between groups tested. Similarly, antipsychotics and sex were added as covariates in all the analyses.

Third, even though we employed an unconventional method to investigate the FC of small thalamic nuclei, we ensured that the thalamic segmentation was precisely aligned to the functional images and we applied more strict inclusion criteria regarding motion with respect to previous studies (93). Moreover, measures of head motion were not correlated with FC values (Table S9). Unfortunately, we did not have longitudinal rs-fMRI data comprising time points before and after the onset of AHs; therefore, our results should be confirmed in a longitudinal sample.

Finally, there are some concerns on a more theoretical level. Despite one of the most consistent findings in patients with schizophrenia being a reduced volume of the mediodorsal nucleus (2), in our sample the mediodorsal nucleus was undamaged. In this regard, some studies support the possibility that mediodorsal nucleus atrophy is state related, that is, the consequence of many years of chronic schizophrenia (52).

In conclusion, we showed that 22qdel carriers have selective alterations of nuclei involved in sensory and cognitive functions. Moreover, 22qdel carriers with AHs exhibit deviant developmental trajectories of the MGN and nuclei playing a pivotal role in memory, accompanied by an immature pattern of thalamocortical connectivity with the AC and speech processing regions. Such augmented connectivity with temporal regions might provide a mechanistic explanation for the predisposition of 22qdel carriers to experience AHs and link it to the neurodevelopmental hypothesis of schizophrenia (105). Therefore, we have demonstrated that thalamic structural and functional abnormalities have the potential role to elucidate complex temporal dynamics on a broader developmental scale, including the deviant comaturation of the thalamus and its cortical targets. Future studies in humans and animal models should further explore the multifaceted developmental interaction between the thalamus and the cortex.

ACKNOWLEDGMENTS AND DISCLOSURES

This work was supported by research grants from the Swiss National Science Foundation (Grant Nos. 324730_121996 and 324730_144260 [to SE]) and a National Centre of Competence in Research Synapsy grant (Grant No. 51NF40-158776 [to SE]). Personal grants from the Swiss National Science Foundation (Grant Nos. PZ00P1_174206 [to MSchn] and 163859 [to MScha]) also supported the current work.

We thank all the families who contributed to the study as well as the family associations (Generation 22, Connect 22, and Relais 22) for their ongoing support. Special thanks go to Virginie Pouillard and Eva Micol for coordinating the project and to the MRI operators at the Center of Biomedical Imaging, Francç is Lazeyras, Lydia Dubourg, and Joëlle van der Molen for their help in scanning.

The authors report no biomedical financial interests or potential conflicts of interest.

ARTICLE INFORMATION

From the Developmental Imaging and Psychopathology Laboratory (VM, DZ, MSchn, MScha, SE) and Department of Genetic Medicine and Development (SE), University of Geneva School of Medicine, Geneva; Clinical Psychology Unit for Developmental and Intellectual Disabilities (MSchn), Faculty of Psychology and Educational Sciences, University of Geneva, Geneva; and Institute of Bioengineering (DZ), École Polytechnique Fédérale de Lausanne, Lausanne, Switzerland; and Department of Neuroscience (MSchn), Center for Contextual Psychiatry, Research Group Psychiatry, KU Leuven, Leuven, Belgium.

Address correspondence to Valentina Mancini, M.D., Developmental Imaging and Psychopathology Laboratory, Campus Biotech, Chemin des Mines 9, 1202 Geneva, Switzerland; E-mail: valentina.mancini@unige.ch.

Received Mar 3, 2020; revised and accepted Apr 23, 2020.

Supplementary material cited in this article is available online at https://doi.org/10.1016/j.bpsc.2020.04.015.

REFERENCES

1. Steullet P (2019): Thalamus-related anomalies as candidate mechanism-based biomarkers for psychosis [published online ahead of print May 27]. Schizophr Res.
2. Pergola G, Selvaggi P, Trizio S, Bertolino A, Blasi G (2015): The role of the thalamus in schizophrenia from a neuroimaging perspective. Neurosci Biobehav Rev 54:57–75.
3. Cronenwett WJ, Csernansky J (2010): Thalamic pathology in schizophrenia. Curr Top Behav Neurosci 4:509–528.
4. Sherman SM (2009): The thalamus is more than just a relay. Curr Opin Neurobiol 17:417–422.
5. Child ND, Benarroch EE (2013): Anterior nucleus of the thalamus: Functional organization and clinical implications. Neurology 81:1869–1876.
6. Sommer IE, Hugdahl K (2019): Auditory hallucinations in schizophrenia: Where are we now and where do we go from here? A personal commentary. Schizophr Res 212:1–3.
7. Waters F, Blom JD, Jardri R, Hugdahl K, Sommer IEC (2018): Auditory hallucinations, not necessarily a hallmark of psychotic disorder. Psychol Med 48:529–536.
8. Diederen KMJ, Daalman K, De Weijer AD, Neggers SFW, Van Gastel W, Blom JD, *et al.* (2012): Auditory hallucinations elicit similar brain activation in psychotic and nonpsychotic individuals. Schizophr Bull 38:1074–1082.
9. Kompus K, Westerhausen R, Hugdahl K (2011): The "paradoxical" engagement of the primary auditory cortex in patients with auditory verbal hallucinations: A meta-analysis of functional neuroimaging studies. Neuropsychologia 49:3361–3369.
10. Braun CMJ, Dumont M, Duval J, Hamel-Hébert I, Godbout L (2003): Brain modules of hallucination: An analysis of multiple patients with brain lesions. J Psychiatry Neurosci 28:432–449.

11. Smith DM, Grant B, Fisher DJ, Borracci G, Labelle A, Knott VJ (2013): Auditory verbal hallucinations in schizophrenia correlate with P50 gating. Clin Neurophysiol 124:1329–1335.
12. Faugère M, Micoulaud-Franchi JA, Boyer L, Cermolacce M, Richieri R, Faget C, *et al.* (2016): Does sensory gating have a protective effect against hallucinatory behavior in schizophrenia? Clin Neurophysiol 127:1746–1748.
13. Thoma RJ, Meier A, Houck J, Clark VP, Lewine JD, Turner J, *et al.* (2017): Diminished auditory sensory gating during active auditory verbal hallucinations. Schizophr Res 188:125–131.
14. Li B, Cui L-B, Xi Y-B, Friston KJ, Guo F, Wang H-N, *et al.* (2017): Abnormal effective connectivity in the brain is involved in auditory verbal hallucinations in schizophrenia. Neurosci Bull 33:281–291.
15. Javitt DC, Sweet RA (2015): Auditory dysfunction in schizophrenia: Integrating clinical and basic features. Nat Rev Neurosci 16:535–550.
16. Allen P, Larøi F, McGuire PK, Aleman A (2008): The hallucinating brain: A review of structural and functional neuroimaging studies of hallucinations. Neurosci Biobehav Rev 32:175–191.
17. Jardri R, Pouchet A, Pins D, Thomas P (2011): Cortical activations during auditory verbal hallucinations in schizophrenia: A coordinate-based meta-analysis. Am J Psychiatry 168:73–81.
18. Zhuo C, Zhu J, Qin W, Qu H, Ma X, Yu C (2017): Cerebral blood flow alterations specific to auditory verbal hallucinations in schizophrenia. Br J Psychiatry 210:209–215.
19. Hoffman RE, Anderson AW, Varanko M, Gore JC, Hampson M (2008): Time course of regional brain activation associated with onset of auditory/verbal hallucinations. Br J Psychiatry 193:424–425.
20. Lennox BR, Park SBG, Medley I, Morris PG, Jones PB (2000): The functional anatomy of auditory hallucinations in schizophrenia. Psychiatry Res 100:13–20.
21. Alderson-day B, Diederen K, Fernyhough C, Ford JM, Horga G, Margulies DS, *et al.* (2016): Auditory hallucinations and the brain's resting-state networks: Findings and methodological observations. Schizophr Bull 42:1110–1123.
22. Chang X, Collin G, Xi Y, Cui L, Scholtens LH, Sommer IE, *et al.* (2017): Resting-state functional connectivity in medication-naïve schizophrenia patients with and without auditory verbal hallucinations: A preliminary report. Schizophr Res 188:75–81.
23. Ferri J, Ford JM, Roach BJ, Turner JA, van Erp TG, Voyvodic J, *et al.* (2018): Resting-state thalamic dysconnectivity in schizophrenia and relationships with symptoms. Psychol Med 48:2492–2499.
24. Cao H, Chén OY, Chung Y, Forsyth JK, McEwen SC, Gee DG, *et al.* (2018): Cerebello-thalamo-cortical hyperconnectivity as a state-independent functional neural signature for psychosis prediction and characterization. Nat Commun 9:3836.
25. Chun S, Westmoreland JJ, Bayazitov IT, Eddins D, Pani AK, Smeyne RJ, *et al.* (2014): Specific disruption of thalamic inputs to the auditory cortex in schizophrenia models. Science 344:1178–1182.
26. van Erp TGM, Hibar DP, Rasmussen JM, Glahn DC, Pearlson GD, Andreassen OA, *et al.* (2016): Subcortical brain volume abnormalities in 2028 individuals with schizophrenia and 2540 healthy controls via the ENIGMA consortium. Mol Psychiatry 21:547–553.
27. Adriano F, Spoletini I, Caltagirone C, Spalletta G (2010): Updated meta-analyses reveal thalamus volume reduction in patients with first-episode and chronic schizophrenia. Schizophr Res 123:1–14.
28. Shepherd AM, Laurens KR, Matheson SL, Carr VJ, Green MJ (2012): Systematic meta-review and quality assessment of the structural brain alterations in schizophrenia. Neurosci Biobehav Rev 36:1342–1356.
29. Ellison-Wright I, Glahn DC, Laird AR, Thelen SM, Bullmore E (2008): The anatomy of first-episode and chronic schizophrenia: An anatomical likelihood estimation meta-analysis. Am J Psychiatry 165:1015–1023.
30. Huang P, Xi Y, Lu ZL, Chen Y, Li X, Li W, *et al.* (2015): Decreased bilateral thalamic gray matter volume in first-episode schizophrenia with prominent hallucinatory symptoms: A volumetric MRI study. Sci Rep 5:14505.
31. Hulshoff Pol HE, Kahn RS (2008): What happens after the first episode? A review of progressive brain changes in chronically ill patients with schizophrenia. Schizophr Bull 34:354–366.
32. Neckelmann G, Specht K, Lund A, Ersland L, Smievoll AI, Neckelmann D, Hugdahl K (2006): MR morphometry analysis of grey matter volume reduction in schizophrenia: Association with hallucinations. Int J Neurosci 116:9–23.
33. Giraldo-Chica M, Woodward ND (2017): Review of thalamocortical resting-state fMRI studies in schizophrenia. Schizophr Res 180:58–63.
34. Cobia DJ, Smith MJ, Salinas I, Ng C, Gado M, Csernansky JG, Wang L (2017): Progressive deterioration of thalamic nuclei relates to cortical network decline in schizophrenia. Schizophr Res 180:21–27.
35. Iglesias JE, Insausti R, Lerma-Usabiaga G, Bocchetta M, Van Leemput K, Greve DN, *et al.* (2018): A probabilistic atlas of the human thalamic nuclei combining ex vivo MRI and histology. NeuroImage 183:314–326.
36. Heilbronner U, Samara M, Leucht S, Falkai P, Schulze TG (2016): The Longitudinal Course of Schizophrenia Across the Lifespan: Clinical, Cognitive, and Neurobiological Aspects. Harv Rev Psychiatry 24:118–128.
37. Fett AJ, Velthorst E, Reichenberg A, Ruggero CJ, Callahan JL, Fochtmann LJ, *et al.* (2019): Long-term Changes in Cognitive Functioning in Individuals With Psychotic Disorders Findings From the Suffolk County Mental Health Project [published online ahead of print Dec 11]. JAMA Psychiatry.
38. Bassett AS, Costain G, Marshall CR (2017): Neuropsychiatric aspects of 22q11.2 deletion syndrome: Considerations in the prenatal setting. Prenat Diagn 37:61–69.
39. McDonald-McGinn DM, Sullivan KE, Marino B, Philip N, Swillen A, Vorstman JAS, *et al.* (2015): 22q11.2 deletion syndrome. Nat Rev Dis Primers 1:15071.
40. Gothelf D, Schneider M, Green T, Debbané M, Frisch A, Glaser B, *et al.* (2013): Risk factors and the evolution of psychosis in 22q11.2 deletion syndrome: A longitudinal 2-site study. J Am Acad Child Adolesc Psychiatry 52:1192–1203.
41. Weisman O, Guri Y, Gur RE, McDonald-McGinn DM, Calkins ME, Tang SX, *et al.* (2017): Subthreshold psychosis in 22q11.2 deletion syndrome: Multisite naturalistic study. Schizophr Bull 43:1079–1089.
42. Tang SX, Yi JJ, Moore TM, Calkins ME, Kohler CG, Whinna DA, *et al.* (2014): Subthreshold psychotic symptoms in 22q11.2 deletion syndrome. J Am Acad Child Adolesc Psychiatry 53:991–1000.e2.
43. Chawner SJRA, Niarchou M, Doherty JL, Moss H, Owen MJ, van den Bree MBM (2019): The emergence of psychotic experiences in the early adolescence of 22q11.2 deletion syndrome. J Psychiatr Res 109:10–17.
44. Debbané M, Glaser B, David MK, Feinstein C, Eliez S (2006): Psychotic symptoms in children and adolescents with 22q11.2 deletion syndrome: Neuropsychological and behavioral implications. Schizophr Res 84:187–193.
45. Mancini V, Sandini C, Padula MC, Zöller D, Schaer M, Eliez S (2019): Positive psychotic symptoms are associated with divergent developmental trajectories of hippocampal volume during late adolescence in patients with 22q11DS [published online ahead of print Jun 3]. Mol Psychiatry.
46. Miller TJ, McGlashan TH, Rosen JL, Cadenhead K, Ventura J, McFarlane W, *et al.* (2003): Prodromal assessment with the Structured Interview for Prodromal Syndromes and the Scale of Prodromal Symptoms: Predictive validity, interrater reliability, and training to reliability. Schizophr Bull 29:703–716.
47. Fischl B, Salat DH, Busa E, Albert M, Dieterich M, Haselgrove C, *et al.* (2002): Whole brain segmentation: Automated labeling of neuroanatomical structures in the human brain. Neuron 33:341–355.
48. Mutlu AK, Schneider M, Debbané M, Badoud D, Eliez S, Schaer M (2013): Sex differences in thickness, and folding developments throughout the cortex. NeuroImage 82:200–207.
49. Whitfield-Gabrieli S, Nieto-Castanon A (2012): Conn: A functional connectivity toolbox for correlated and anticorrelated brain networks. Brain Connect 2:125–141.
50. Tousignant B, Eugène F, Sirois K, Jackson PL (2018): Difference in neural response to social exclusion observation and subsequent altruism between adolescents and adults. Neuropsychologia 116:15–25.

51. Cho KIK, Kwak Y Bin, Hwang WJ, Lee J, Kim M, Lee TY, Kwon JS (2019): Microstructural changes in higher-order nuclei of the thalamus in patients with first-episode psychosis. Biol Psychiatry 85:70–78.
52. Pergola G, Trizio S, Di Carlo P, Taurisano P, Mancini M, Amoroso N, *et al.* (2017): Grey matter volume patterns in thalamic nuclei are associated with familial risk for schizophrenia. Schizophr Res 180:13–20.
53. Bish JP, Nguyen V, Ding L, Ferrante S, Simon TJ (2004): Thalamic reductions in children with chromosome 22q11.2 deletion syndrome. NeuroReport 15:1413–1415.
54. Larsen KM, Dzafic I, Siebner HR, Garrido MI (2019): Alteration of functional brain architecture in 22q11.2 deletion syndrome—Insights into susceptibility for psychosis. NeuroImage 190:154–171.
55. Baker K, Baldeweg T, Sivagnanasundaram S, Scambler P, Skuse D (2005): COMT $Val^{108/158}$Met Modifies Mismatch Negativity and Cognitive Function in 22q11 Deletion Syndrome. Biol Psychiatry 58:23–31.
56. Zarchi O, Carmel M, Avni C, Attias J, Frisch A, Michaelovsky E, *et al.* (2013): Schizophrenia-like neurophysiological abnormalities in 22q11.2 deletion syndrome and their association to COMT and PRODH genotypes. J Psychiatr Res 47:1623–1629.
57. Rihs TA, Tomescu MI, Britz J, Rochas V, Custo A, Schneider M, *et al.* (2013): Altered auditory processing in frontal and left temporal cortex in 22q11.2 deletion syndrome: A group at high genetic risk for schizophrenia. Psychiatry Res 212:141–149.
58. Attout L, Noël M, Vossius L, Rousselle L (2017): Evidence of the impact of visuo-spatial processing on magnitude representation in 22q11.2 microdeletion syndrome. Neuropsychologia 99:296–305.
59. Bostelmann M, Schneider M, Padula MC, Maeder J, Schaer M, Scariati E, *et al.* (2016): Visual memory profile in 22q11. 2 microdeletion syndrome: Are there differences in performance and neurobiological substrates between tasks linked to ventral and dorsal visual brain structures? A cross-sectional and longitudinal study. J Neurodev Disord 8:41.
60. Saalmann YB, Pinsk MA, Wang L, Li X, Kastner S (2013): Pulvinar regulates information transmission between cortical areas based on attention demands. Science 337:753–756.
61. Allen AE, Procyk CA, Howarth M, Walmsley L, Brown TM (2016): Visual input to the mouse lateral posterior and posterior thalamic nuclei: Photoreceptive origins and retinotopic order. J Physiol 7:1911–1929.
62. Sobin C, Kiley-Brabeck K, Karayiorgou M (2005): Associations between prepulse inhibition and executive visual attention in children with the 22q11 deletion syndrome. Mol Psychiatry 10:553–562.
63. Bish JP, Chiodo R, Mattei V, Simon TJ (2007): Domain specific attentional impairments in children with chromosome 22q11.2 deletion syndrome. Brain Cogn 64:265–273.
64. Homman-Ludiye J, Mundinano IC, Kwan WC, Bourne JA (2020): Extensive connectivity between the medial pulvinar and the cortex revealed in the marmoset monkey. Cereb Cortex 30:1797–1812.
65. Homman-Ludiye J, Bourne JA (2019): The medial pulvinar: Function, origin and association with neurodevelopmental disorders. J Anat 235:507–520.
66. Boot E, Butcher NJ, van Amelsvoort AMJ, Lang AE, Marras C, Pondal M, *et al.* (2015): Movement disorders and other motor abnormalities in adults with 22q11.2 deletion syndrome. Am J Med Genet A 167:639–645.
67. Butcher NJ, Boot E, Lang AE, Andrade D, McDonald-mcGinn JVD, Bassett AS (2018): Neuropsychiatric expression and catatonia in 22q11.2 deletion syndrome: An overview and case series. Am J Med Genet A 176:2146–2159.
68. Van der Werf YD, Witter MP, Groenewegen HJ (2002): The intralaminar and midline nuclei of the thalamus: Anatomical and functional evidence for participation in processes of arousal and awareness. Brain Res Brain Res Rev 39:107–140.
69. Maeder J, Schneider M, Bostelmann M, Debbané M, Glaser B, Menghetti S, *et al.* (2016): Developmental trajectories of executive functions in 22q11.2 deletion syndrome. J Neurodev Disord 8:10.
70. Jones EG, Rubenstein JLR (2004): Expression of regulatory genes during differentiation of thalamic nuclei in mouse and monkey. J Comp Neurol 477:55–80.
71. Nakagawa Y (2019): Development of the thalamus: From early patterning to regulation of cortical functions. Wiley Interdiscip Rev Dev Biol 8:e345.
72. Meng Q, Wang K, Brunetti T, Xia Y, Jiao C, Dai R, *et al.* (2018): The DGCR5 long noncoding RNA may regulate expression of several schizophrenia-related genes. Sci Transl Med 10:eaat6912.
73. Warland A, Kendall KM, Rees E, Kirov G, Caseras X (2020): Schizophrenia-associated genomic copy number variants and subcortical brain volumes in the UK Biobank. Mol Psychiatry 25:854–862.
74. Dolleman-van der Weel MJ, Griffin AL, Ito HT, Shapiro ML, Witter MP, Vertes RP, Allen TA (2019): The nucleus reuniens of the thalamus sits at the nexus of a hippocampus and medial prefrontal cortex circuit enabling memory and behavior. Learn Mem 26:191–205.
75. Hallock HL, Wang A, Griffin AL (2016): Ventral midline thalamus is critical for hippocampal-prefrontal synchrony and spatial working memory. J Neurosci 36:8372–8389.
76. Lisman JE, Pi HJ, Zhang Y, Otmakhova NA (2010): A thalamo-hippocampal-ventral tegmental area loop may produce the positive feedback that underlies the psychotic break in schizophrenia. Biol Psychiatry 68:17–24.
77. Mukherjee A, Carvalho F, Eliez S, Caroni P, Mukherjee A, Carvalho F, *et al.* (2019): Long-lasting rescue of network and cognitive dysfunction in a genetic schizophrenia model article long-lasting rescue of network and cognitive dysfunction. Cell 178:1387–1402.e14.
78. Dumont JR, Amin E, Poirier GL, Albasser MM, Aggleton JP (2012): Anterior thalamic nuclei lesions in rats disrupt markers of neural plasticity in distal limbic brain regions. Neuroscience 224:81–101.
79. Mesulam M, Thompson CK, Weintraub S, Rogalski EJ (2015): The Wernicke conundrum and the anatomy of language comprehension in primary progressive aphasia. Brain 138:2423–2437.
80. Gong J, Luo C, Li X, Jiang S, Khundrakpam BS, Duan M, *et al.* (2019): Evaluation of functional connectivity in subdivisions of the thalamus in schizophrenia. Br J Psychiatry 214:288–296.
81. Woodward ND, Heckers S (2016): Mapping thalamocortical functional connectivity in chronic and early stages of psychotic disorders. Biol Psychiatry 79:1016–1025.
82. Schleifer C, Lin XA, Kushan L, Ji XJL, Yang G, Bearden XCE (2019): Dissociable disruptions in thalamic and hippocampal resting-state functional connectivity in youth with 22q11.2 deletions. J Neurosci 39:1301–1319.
83. Kumari V, Fannon D, Dominic H, Raveendran V, Antonova E, Premkumar P, *et al.* (2010): Functional MRI of verbal self-monitoring in schizophrenia: Performance and illness-specific effects. Schizophr Bull 36:740–755.
84. Spencer KM (2012): Baseline gamma power during auditory steady-state stimulation in schizophrenia. Front Hum Neurosci 5:190.
85. Raichle ME, MacLeod AM, Snyder AZ, Powers WJ, Gusnard DA, Shulman GL (2001): A default mode of brain function. Proc Natl Acad Sci U S A 98:676–682.
86. Gusnard DA, Raichle ME, Raichle ME (2001): Searching for a baseline: Functional imaging and the resting human brain. Nat Rev Neurosci 2:685–694.
87. Mattiaccio LM, Coman IL, Schreiner MJ, Antshel KM, Fremont WP, Bearden CE, Kates WR (2016): Atypical functional connectivity in resting-state networks of individuals with 22q11.2 deletion syndrome: Associations with neurocognitive and psychiatric functioning. J Neurodev Disord 8:2.
88. Gabrieli JDE, Seidman LJ (2009): Hyperactivity and hyperconnectivity of the default network in schizophrenia and in first-degree relatives of persons with schizophrenia. Proc Natl Acad Sci U S A 106:1279–1284.
89. Broyd SJ, Demanuele C, Debener S, Helps SK, James CJ, Sonuga-barke EJS (2009): Default-mode brain dysfunction in

mental disorders: A systematic review. Neurosci Biobehav Rev 33:279–296.

90. Pomarol-Clotet E, Salvador R, Sarro S, Gomar J, Vila F, Guerrero A, *et al.* (2008): Failure to deactivate in the prefrontal cortex in schizophrenia: Dysfunction of the default mode network? Psychol Med 38:1185–1193.
91. Debbané M, Lazouret M, Lagioia A, Schneider M, Ville D Van De, Eliez S (2012): Resting-state networks in adolescents with 22q11.2 deletion syndrome: Associations with prodromal symptoms and executive functions. Schizophr Res 139:33–39.
92. Schreiner MJ, Karlsgodt KH, Uddin LQ, Chow C, Congdon E, Jalbrzikowski M, Bearden CE (2014): Default mode network connectivity and reciprocal social behavior in 22q11.2 deletion syndrome. Soc Cogn Affect Neurosci 9:1261–1267.
93. Zöller D, Schaer M, Scariati E, Padula MC, Eliez S, Van De Ville D (2017): Disentangling resting-state BOLD variability and PCC functional connectivity in 22q11.2 deletion syndrome. NeuroImage 149:85–97.
94. Padula MC, Schaer M, Scariati E, Schneider M, Van De Ville D, Debbané M, Eliez S (2015): Structural and functional connectivity in the default mode network in 22q11.2 deletion syndrome. J Neurodev Disord 7:23.
95. Northoff G, Qin P (2011): How can the brain's resting state activity generate hallucinations? A "resting state hypothesis" of auditory verbal hallucinations. Schizophr Res 127:202–214.
96. Northoff G (2014): Are auditory hallucinations related to the brain's resting state activity? A "neurophenomenal resting state hypothesis". Clin Psychopharmacol Neurosci 12:189–195.
97. Honey CJ, Sporns O, Cammoun L, Gigandet X, Thiran JP, Meuli R, Hagmann P (2009): Predicting human resting-state functional connectivity. Proc Natl Acad Sci U S A 106:2035–2040.
98. Zhang D, Snyder AZ, Fox MD, Sansbury MW, Shimony JS, Raichle ME (2008): Intrinsic functional relations between human cerebral cortex and thalamus. J Neurophysiol 100:1740–1748.
99. Fair DA, Bathula D, Mills KL, Dias TGC, Blythe MS, Margulies D (2010): Maturing thalamocortical functional connectivity across development. Front Syst Neurosci 4:10.
100. Zagrebelsky M, Bandtlow CE, Schwab ME, Korte M (2010): Nogo-A stabilizes the architecture of hippocampal neurons. J Neurosci 30:13220–13234.
101. Masanori I, Tanigaki K, Muraki K, Miyata J, Takemura AT, Fukuyama H, *et al.* (2015): Polymorphism within a neuronal activity-dependent enhancer of NgR1 is associated with corpus callosum morphology. Mol Psychiatry 8524:105–115.
102. Modinos G, Costafreda SG, van Tol MJ, McGuire PK, Aleman A, Allen P (2013): Neuroanatomy of auditory verbal hallucinations in schizophrenia: A quantitative meta-analysis of voxel-based morphometry studies. Cortex 49:1046–1055.
103. Chow EWC, Ho A, Wei C, Voormolen EHJ, Crawley AP, Bassett AS (2011): Association of schizophrenia in 22q11.2 deletion syndrome and gray matter volumetric deficits in the superior temporal gyrus. Am J Psychiatry 168:522–529.
104. Schmitt JE, Vandekar S, Yi J, Calkins ME, Ruparel K, Roalf DR, *et al.* (2015): Aberrant cortical morphometry in the 22q11.2 deletion syndrome. Biol Psychiatry 78:135–143.
105. Insel TR (2010): Rethinking schizophrenia. Nature 468:187–193.